Characteristics of Electron Heat Transport of Plasma with an Electron Internal-Transport Barrier in the Large Helical Device

K. Ida,[1] T. Shimozuma,[1] H. Funaba,[1] K. Narihara,[1] S. Kubo,[1] S. Murakami,[2] A. Wakasa,[3] M. Yokoyama,[1] Y. Takeiri,[1] K. Y. Watanabe,[1] K. Tanaka,[1] M. Yoshinuma,[1] Y. Liang,[1] N. Ohyabu,[1] and LHD experimental group[1]

[1]*National Institute for Fusion Sciences, Toki, Gifu 509-5292, Japan*
[2]*Department of Nuclear Engineering, Kyoto University, Kyoto 606-8501, Japan*
[3]*Graduate School of Engineering, Hokkaido University, Sapporo 060-8628, Japan*

(Received 11 January 2003; published 19 August 2003)

Associated with the transition from ion root to electron root, an electron internal transport barrier (ITB) appears in the large helical device, when the heating power of electron cyclotron resonance heating exceeds the threshold power. The incremental thermal diffusivity of electron heat transport χ_e^{inc} in the ITB plasma is much lower than that in the plasma with the heating power below the threshold, and the thermal diffusivity χ_e decreases with increasing of heating power $[d\chi_e/d(P/n_e) < 0]$ in helical ITB plasmas.

DOI: 10.1103/PhysRevLett.91.085003 PACS numbers: 52.55.Hc, 52.50.Gj

Recently, the electron thermal transport barrier has been observed with dominant electron cyclotron heating in the plasma with a negative magnetic field shear in many tokamaks [1–6]. In these experiments, the radial profiles of the rotational transform (safety factor) are measured or calculated and the role of the magnetic shear in the formation of electron internal transport barrier is discussed and the role of the radial electric field E_r shear on the electron and ion transport barrier has been studied in tokamak plasma [7,8]. On the other hand, in a stellarator, where the magnetic shear is negative, the electron internal transport barrier (ITB) has been observed associated with the transition from ion root (large neoclassical flux with a small E_r) to electron root (small neoclassical flux with a large positive E_r), when the collisionality becomes low enough for the transition [9–11]. Although the mechanism of ITB formation associated with the transition from ion root to electron root has been studied [10,11], the characteristics of thermal transport, i.e., the relation between electron temperature gradient ∇T_e and heat flux normalized by electron density Q/n_e, have not been studied quantitatively. A quantitative comparison of electron thermal diffusivity χ_e $[= (Q/n_e)/\nabla T_e]$ and an incremental electron thermal diffusivity χ_e^{inc} $[= d(Q/n_e)/d(\nabla T_e)]$ has not been done in ITB plasma in helical devices in spite of its importance in understanding the transport in toroidal devices [12]. In the L-mode plasma, the instability, such as electron temperature gradient mode [13,14], often results in the sharp increase of the thermal diffusivity above the critical electron temperature gradients and determines the upper limit of the electron temperature for the available heating power [15]. Therefore, the dependence of the thermal diffusivity on the temperature gradient is an extremely important issue to have a prospect of the plasma performance with an electron ITB in the high temperature regime required for nuclear fusion. Once the ITB is achieved, it is more important how the thermal diffusivity changes as the heating power is increased than how much is the reduction of thermal diffusivity at the transition from the L-mode plasma to the ITB plasma. The incremental thermal diffusivity χ_e^{inc} is a key parameter in this study, because the dependence of thermal diffusivity on heating power P (sign of $d\chi_e/dP$) is determined by the ratio of two thermal diffusivities ($\chi_e^{\mathrm{inc}}/\chi_e < 1$ or > 1). In this Letter, the relation between the T_e gradient and heat flux, especially incremental χ_e^{inc} in the plasma with ITB at significant low collisionality regime ($\nu_b^* < 0.2$, where ν_b^* is electron collisionality normalized by bounce frequency of banana orbit), are discussed.

The large helical device (LHD) is a toroidal helical magnetic device (Heliotron device) with a major radius of $R_{\mathrm{ax}} = 3.5$–4.1 m, an average minor radius of 0.6 m, and magnetic field B of 0.5–3 T. The radial profiles of E_r are derived from poloidal flow velocity v_θ measured with charge exchange spectroscopy at the mid plane in LHD by using a charge exchange reaction between fully ionized neon (0.5%–1%) impurity and atomic hydrogen from the neutral beam [16,17]. The contribution of toroidal flow velocity and pressure gradient of neon to the radial electric field are negligibly small (0.3 and 0.1 kV/m, respectively), because of damping of toroidal flow and higher charge of impurity measured. Three neutral beams with the beam energy of 130–145 keV and absorbed power of 1.3 MW are injected from 0.3 to 3.3 s to initiate and sustain the plasma and electron cyclotron resonance heating (ECH) in the 2nd harmonic resonance with the frequency of 82.7 and 84 GHz and with the power of 0.63–0.88 MW is added for $t = 1.7$–2.2 s. The focal point of ECH [18] is tuned exactly at the magnetic axis R_{ax} of 3.8 m (major radius in vacuum R_{ax}^v of 3.75 m), which is measured with a soft x-ray charge-coupled device camera

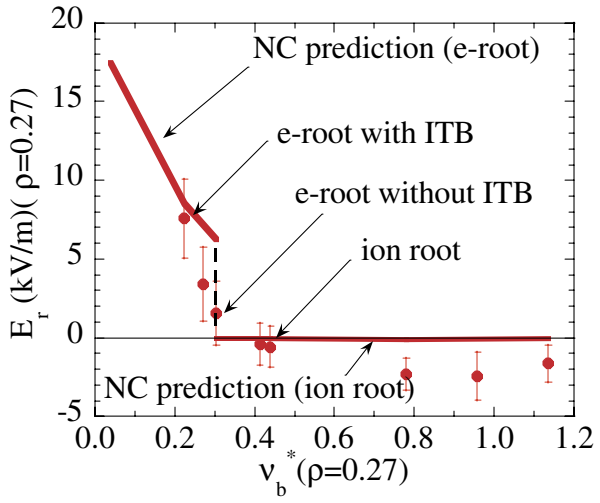

FIG. 1 (color online). E_r as a function of normalized electron collisionality ν_b^* at $\rho = 0.27$ with the magnetic field of 1.52 T and with the magnetic axis of 3.8 m.

[19]. The transition from ion root to electron root is observed near the plasma center with localized ECH when the plasma is well into the collisionless regime ($\nu_b^* < 0.3$) by decreasing electron density as shown in Fig. 1. The transition phenomena from ion root to electron root are quite similar to that observed in a compact helical system (CHS). The neoclassical (NC) prediction using diffusion coefficient calculation by Monte Carlo method (DCOM) code [20] shows good agreement with the measurements in the critical collisionality for the transition of E_r. According to the global neoclassical transport simulation (GNET) code [21] calculation, the nonambipolar electron flux of energetic electrons driven by ECH is only 30% of the electron neoclassical flux for the plasma parameter in this experiment and the neoclassical flux dominates the ambipolar condition. However, the effect of the direct electron loss driven by ECH should be taken into account in the calculation of E_r at lower electron density.

When the plasma collisionality is low enough ($\nu_b^* = 0.2$ at $\rho = 0.27$) for the transition of ion root to electron root, the formation of an electron internal transport barrier is observed for the plasma with ECH power above the threshold. Figure 2 shows the radial profiles of rotational transform ($\iota = 1/q$, where q is the safety factor) and electron density measured with the far-infrared laser interferometer, T_e measured with YAG Thomson scattering (averaged with four time slices), ion temperature and E_r measured with charge exchange spectroscopy, and χ_e and normalized χ_e for the plasmas with ECH power above the threshold (0.78 MW) and below the threshold (0.58 MW). A smoothed curve with a function of $c_1 + c_2\rho^2 + c_3 \exp(-\rho^2/c_4^2)$ for the transport analysis, where c_1–c_4 are fitting parameters, are also plotted. The profiles of the plasma without additional ECH are also plotted as a reference. The central electron density drops slightly due to the poor confinement of perpendicularly accelerated electrons by ECH (pump out effect) and central T_e increases only less than 30% (from 1.72 to 2.18 keV) for the ECH power of 0.58 MW. However, when the ECH power exceeds the power threshold, the central T_e increases significantly and a large temperature gradient appears near the plasma center at $\rho < 0.3$, while there is not much change observed in the profiles in electron density, rotational transform ι, and ion temperature. The transition of E_r from a small positive value to the large positive value is observed at $\rho < 0.4$ when the ECH power exceeds the threshold. There is no transition of E_r and increase of temperature gradient regardless of the ECH power when the collisionality $\nu_b^*(\rho = 0.27)$ is larger than 0.3. Although there is a significant observed increase of T_e, no increase of ion temperature is observed [Fig. 2(c)], which is in contrast to the formation of both ion and electron transport barrier in ECH-driven ITB plasma in CHS, where the heating power to ions is comparable to that to electrons because of the lower energy of neutral-beam injection (NBI) (30–40 keV). No increase of ion temperature in LHD would be because the growth rate of a long wavelength turbulence contributing the ion heat transport is enhanced due to the increase of the ratio of T_e/T_i. (The degradation of ion transport associated with the increase of T_e/T_i ratio is often observed [22–24]). The E_r near the plasma center changes its sign from negative to positive when the ECH is applied to the plasma center. However, the magnitudes of E_r and its shear are small when there is no internal transport barrier. The strong E_r and its shear appear associated with the formation of the ITB [Fig. 2(d)], which is qualitatively predicted by the transport model including neoclassical and anomalous transport in helical plasmas [25]. Transport analysis shows the clear reduction of χ_e associated with the formation of ITB at $\rho < 0.3$ [Figs. 2(e) and 2(f)]. The fact that the χ_e measured is still higher than the prediction by neoclassical theory shows that the formation of the ITB is due to the reduction of the electron heat transport driven by a short wavelength turbulence not due to the neoclassical transport. It should be noted that the absolute values of χ_e predicted by neoclassical theory are even larger for the plasma with an ITB. This is because the increase of E_r is not enough to compensate for the increase of ripple loss due to the higher T_e. Since the electron transport in these plasmas are considered to be governed by the turbulent transport, the χ_e measured are normalized by $T_e^{3/2}$ in Fig. 2(f). The χ_e normalized by the gyro-Bohm factor $T_e^{3/2}$ is considered to be roughly constant in the L-mode plasmas when the temperature gradient is below the threshold of the normalized temperature gradient R/L_{Te}, where R is the major radius and L_{Te} is the scale length of the T_e radial profile [15]. The normalized χ_e in the ECH + NBI heated plasma with an ITB is lower than the plasma with NBI heating inside the transport barrier at $\rho < 0.3$.

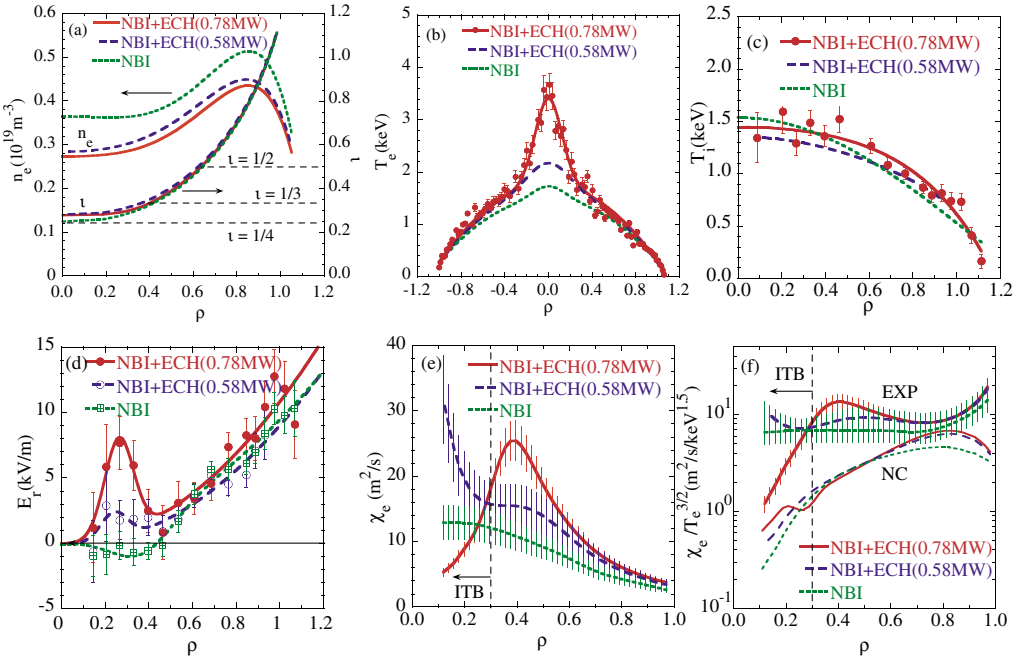

FIG. 2 (color online). Radial profiles of (a) electron density, rotational transform ι, (b) electron temperature, (c) ion temperature, (d) radial electric field, (e) χ_e, and (f) χ_e normalized by $T_e^{3/2}$ measured and predicted by NC theory for the plasma with ECH above the threshold (shot 32940) and below the threshold (shot 32942) for the formation of ITB with the magnetic field of 1.52 T and with the magnetic axis of 3.8 m. The profiles of the plasma without ECH are also plotted as a reference.

It is important to study the electron transport for the plasma with an ITB at much lower collisionality ($\nu_b^* \sim 0.03$), where the neoclassical heat transport due to the helical ripple loss would be serious. In order to achieve a plasma with lower collisionality, the electron density is reduced to 0.14×10^{19} m^{-3}, which is lower than the critical electron density for the transition of E_r by a factor of 3. As the electron density decreases, the central electron temperature increases sharply up to 8 keV. The maximum of the normalized T_e gradient (R/L_{Te}) jumps from 6 to 23 in the regime of transition and increases from 23 to 30 after the formation of the ITB. As shown in Fig. 3(a), the density dependence of the central T_e in the L mode ($n_e < 0.5 \times 10^{19}$ m^{-3}) is $n_e^{-0.43}$, which is consistent to that predicted by the L-mode scaling of $T_e(0) \propto n_e^{-0.39}$ in LHD [26] and also consistent with gyro-reduced Bohm transport [$T_e(0) \propto n_e^{-0.4}$]. It should be noted that in the regime of the improved mode ($n_e < 0.5 \times 10^{19}$ m^{-3}) the density dependence of the central T_e is $T_e(0) \propto n_e^{-0.6}$, which is much stronger than that in the L mode. The formation of the electron internal transport barrier is due to the bifurcation phenomena of the electron heat transport, which is clearly demonstrated in the relation between the electron heat flux normalized by density and

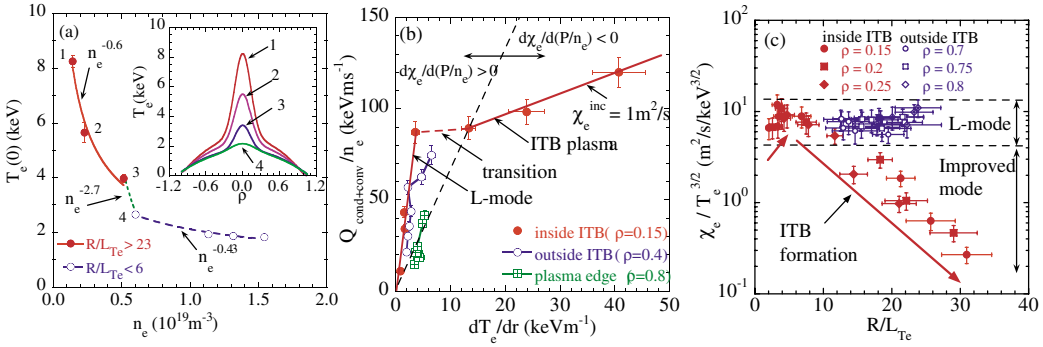

FIG. 3 (color online). (a) Central electron temperature T_e as a function of line averaged electron density (shots 32958, 32957, 32940, 32942, 32968, 32970, and 32971). (b) Electron heat flux normalized by the electron density as a function of the temperature gradient at various averaged minor radii ρ and (c) normalized heat diffusivity measured as a function of R/L_{Te} inside (open symbols) and outside (closed symbols) the internal transport barrier.

temperature gradient as seen in Fig. 3(b). At the transition from an L-mode plasma to the ITB plasma, the T_e gradient near the plasma center ($\rho = 0.15$) jumps from 3.6 to 13 keV/m even for the same magnitude of heat flux (reduction of χ_e by a factor of 4). After the transition to an ITB plasma, χ_e decreases up to 3 m^2/s (reduction of χ_e by a factor of 8). The incremental thermal diffusivity $\chi_e^{\rm inc}$ in ITB plasma near the plasma center ($\rho = 0.15$) is 1 m^2/s, which is lower than that for the plasma without ITB by a factor of 20. Because of $\chi_e^{\rm inc} < \chi_e$ inside the ITB, the χ_e decreases as the normalized heat flux or heating power is increased [$d\chi_e/d(P/n_e) < 0$], which can be called "power confinement enhancement" in contrast to the power confinement degradation in the L-mode plasma or outside ITB. If the $\chi_e^{\rm inc}$ in ITB plasma is larger than the χ_e just after the transition [dashed line in Fig. 3(b)], the χ_e increases as the heating power is increased [$d\chi_e/d(P/n_e) > 0$].

In order to evaluate the reduction of the electron heat transport quantitatively, the χ_e is normalized by $T_e^{3/2}$ as plotted in Fig. 3(c). When there is no ITB in the plasma, the normalized χ_e near the plasma center ($\rho =$ 0.15–0.25) and edge ($\rho = 0.7$–0.8) are at L-mode levels (5–12 $m^2\,s^{-1}\,keV^{-3/2}$). After the formation of an ITB, the normalized χ_e inside the ITB decreases up to 0.3 $m^2\,s^{-1}\,keV^{-3/2}$ as the normalized temperature gradient R/L_{Te} increases to 30, which is comparable to that observed in an internal transport barrier in tokamaks. In contrast to that, the normalized χ_e near the edge stays constant as R/L_{Te} increases. The symptom of the increase of normalized χ_e at $R/L_{Te} \sim 20$ implies the existence of turbulent transport with a threshold in R/L_{Te} near the plasma edge, while the normalized χ_e near the center significantly exceeds the critical value after the formation of the ITB. The critical normalized temperature gradient for the formation of the ITB (R/L_{Te} at the maximum χ_e) is small (~ 3) near the plasma center, where the magnetic shear is weak [$s/q = 0.2$ at $\rho = 0.2$, where $s = (r/q)(\partial q/\partial r)$], while it becomes large (~ 20) near the plasma edge where the magnetic shear is high ($s/q =$ 1.4 at $\rho = 0.75$). These observations show that there is a similarity in LHD and tokamaks in the dependence of threshold in R/L_{Te} on magnetic shear (~ 5 at $s/q = 0.1$ and ~ 13 at $s/q = 0.7$) [27].

It is interesting that the electron transport barrier is observed in the magnetic field configurations with negative shear (reversed shear in a tokamak and normal shear in Heliotron). This fact shows the importance of the negative shear for the formation of the electron ITB. There are some differences in the characteristics of the electron ITB between tokamak and Heliotron plasmas. The transport barrier tends to be localized near the minimum q and the χ_e increases (flattening of the temperature profile is sometimes observed) near the magnetic axis, especially when the central q is large ~ 6 ($\iota \sim 0.16$) in tokamak [1]. However, there is no increase of χ_e towards the magnetic axis observed in LHD. This is because the rotational transform is large enough ($\iota \sim 0.3$) to sustain the good confinement. The transition to the electron root, where the E_r is strongly linked with the dT_e/dr, is the key in the formation of an ITB in a Heliotron, while the reversed shear is important in a tokamak.

In conclusion, a clear transition phenomena in the electron heat flux is observed associated with the transition from the ion root to the electron root in the LHD plasmas. The transport analysis shows that the $\chi_e^{\rm inc}$ in the plasma with ITB is 1 m^2/s, which is much lower than that without ITB by more than 1 order of magnitude. Because of $\chi_e^{\rm inc} < \chi_e$, the χ_e decreases as the heat flux is increased inside the ITB (power confinement enhancement). The χ_e normalized by $T_e^{3/2}$ drops to 0.3 $m^2/s/keV^{3/2}$ at the highest gradient of $R/L_{Te} < 30$.

The authors thank Dr. A. Fujisawa, Dr. H. Sanuki, Dr. K. Itoh, and Dr. T. Fukuda (JAERI) for useful discussions and the technical support on LHD for the experiments. This work is partly supported by a grant-in-aid for scientific research of MEXT Japan.

[1] T. Fujita *et al.*, Phys. Rev. Lett. **78**, 2377 (1997).
[2] M. R. de Baar *et al.*, Phys. Rev. Lett. **78**, 4573 (1997).
[3] P. Buratti *et al.*, Phys. Rev. Lett. **82**, 560 (1999).
[4] S. Gunter *et al.*, Phys. Rev. Lett. **84**, 3097 (2000).
[5] Z. A. Pietrzyk *et al.*, Phys. Rev. Lett. **86**, 1530 (2001).
[6] C. D. Challis *et al.*, Plasma Phys. Controlled Fusion **43**, 861 (2001).
[7] B. W. Stallard *et al.*, Phys. Plasmas **6**, 1978 (1999).
[8] L. L. Lao *et al.*, Phys. Plasmas **3**, 1951 (1996).
[9] H. Idei *et al.*, Phys. Rev. Lett. **71**, 2220 (1993).
[10] A. Fujisawa *et al.*, Phys. Rev. Lett. **82**, 2669 (1999).
[11] U. Stroth *et al.*, Phys. Rev. Lett. **86**, 5910 (2001).
[12] F. Wagner and U. Stroth, Plasma Phys. Controlled Fusion **35**, 1321 (1993).
[13] W. Dorland *et al.*, Phys. Rev. Lett. **85**, 5579 (2000).
[14] J. Q. Dong *et al.*, Phys. Plasmas **9**, 4699 (2002).
[15] F. Ryter *et al.*, Plasma Phys. Controlled Fusion **43**, A323 (2001).
[16] K. Ida *et al.*, Rev. Sci. Instrum. **71**, 2360 (2000).
[17] K. Ida *et al.*, Phys. Rev. Lett. **86**, 5297 (2001).
[18] S. Kubo *et al.*, J. Plasma Fusion Res. **78**, 99 (2002).
[19] Y. Liang *et al.*, Plasma Phys. Controlled Fusion **44**, 1383 (2002).
[20] A. Wakasa *et al.*, J. Plasma Fusion Res. SERIES **4**, 408 (2001).
[21] S. Murakami *et al.*, Nucl. Fusion **40**, 693 (2000).
[22] C. C. Petty *et al.*, Phys. Rev. Lett. **83**, 3661 (1999).
[23] S. Ide *et al.*, Plasma Phys. Controlled Fusion **44**, A137 (2002)
[24] K. Ida *et al.*, Plasma Phys. Controlled Fusion **40**, 793 (1998).
[25] S. Toda *et al.*, Plasma Phys. Controlled Fusion **44**, A501 (2002).
[26] H. Yamada *et al.*, Phys. Rev. Lett. **84**, 1216 (2000).
[27] G. T. Hoang *et al.*, Phys. Rev. Lett. **87**, 125001 (2001).